Nonlinear Dynamics and Systems Theory, **9** (4) (2009) 433–442

Residual Generator Based Measurement of Current Input Into a Cell

K. Röbenack *

Institut für Regelungs- und Steuerungstheorie, Fakultät Elektrotechnik und Informationstechnik, Technische Universität Dresden, 01062 Dresden, Germany.

Received: July 30, 2008; Revised: September 8, 2009

Abstract: We address the problem of real-time estimation of the excitation current into a cell. The membrane voltages can be measured experimentally, even in vivo. On the other hand, a direct measurement of the current into a cell interferes with the voltage activity. We propose a method to estimate the current input into a cell using the measured voltage and an observer based residual generator scheme. Our approach can be applied to all cell models of the Hodgkin-Huxley type.

Keywords: *cell models; observer; residual generator; nonlinear control.*

Mathematics Subject Classification (2000): 92C37, 93B30, 93C10, 93D25.

1 Introduction

The paper addresses a measurement problem from cell biology. In particular, the potential on the membrane of a cell such as a neuron can be recorded directly via voltage measurement. The electrophysiological behaviour of the cell, especially the membrane voltage dynamics, is influenced by ionic channels which allow ions to move through the cell's membrane.

Voltage clamp is a standard method to measure ionic currents across a membrane [1, 2]. The technique developed by Cole [3] uses two electrodes. One electrode is used to measure the intracellular voltage relative to ground. This voltage is amplified and compared with a given reference voltage. The difference of these signals is amplified again and feed back via the second electrode. With this feedback the potential on the membrane is hold at a specific level. The current injected into the cell by this feedback

* Corresponding author: klaus@roebenack.de

structure compensates the ionic current, i.e., the output current of the second amplifier has equal value but opposite sign of the ionic current.

During the last decades, several more advanced measurement techniques such as patch clamp [4] have been developed, see [5,6] and references cited there. Unfortunately, most measurement methods have at least one the following disadvantages: measurement inferences with the cell's activities, or requirement of very specific laboratory conditions (limiting the applicability in vivo), or expensive measurement devices, or slow dynamics.

The author suggests a new technique for a real-time estimation of the current input into a cell. The paper extends preliminary results published in [7, 8]. Our approach requires a dynamical model describing the interaction between the membrane voltage and the different kinds of current. To estimate the input current we use an observer based residual generator. The usage of an observer to estimate quantities which are not directly available for measurement is quite common in system and control theory [9]. Originally, residual generators are used to detect the occurence of faults in a given system [10]. Here, we apply such a generator to reconstruct the input current quantitatively.

In Section 2 we present a large class of cell models. An observer based method to estimate the current input into a cell is derived in Section 3. Our estimation scheme is used in Section 4 to reconstruct the input current for the Hudgkin–Huxley model of a neuron.

2 Cell Models

2.1 Conductance-based models

Important aspects of the biophysical behaviour of an excitable cell such as a neuron can be represented by an equivalent circuit model. The dynamics of the membrane voltage V is governed by a differential equation

$$C\dot{V} = I - \sum_j \widetilde{g}_j \, (V - V_j) \tag{2.1}$$

with a capacitance $C > 0$. The current I is injected into the cell, either from a coupling with other cells, or by an electrode. The sum in (2.1) represents the ionic currents, that is the leak current and the currents flowing through ionic channels. The reversal potential of the ith channel is denoted by V_i. The ionic channels, which describe the concentrations of certain ions, have two states: open and closed. The probability of a channel to be open is represented by a so-called gating variable. In particular, the conductances $\widetilde{g}_j$ may depend on some gating variables. The dynamics of the gating variables $w_1, \ldots, w_p$ is governed by differential equations of the form

$$\dot{w}_i = \alpha_i(V)\,(1 - w_i) - \beta_i(V) w_i \quad \text{for} \quad i = 1, \ldots, p \tag{2.2}$$

with functions α_i and β_i. These functions result from the Markov model of the associated ionic channel (see [11]). More precisely, the functions α_i and β_i are the transition rates for opening and closing an channel. Furthermore, we have $\alpha_i(V), \beta_i(V) > 0$ for all V.

2.2 Hodgkin–Huxley model

The most well-known simulation model for excitable cells such as neurons and cardiac myocytes was developed by Hodgkin and Huxley [12]. Originally, the model describes

the ionic mechanisms underlying the initiation and propagation of action potentials in the squid giant axon. The model takes the concentrations of sodium ions (Na^+) and potassium ions (K^+) into account. In this case, Eq. (2.1) becomes

$$C\dot{V} = I - I_{Na} - I_K - I_L \tag{2.3}$$

with $C = 1\mu\text{F/cm}^2$. The ionic currents I_{Na} and I_K, and the leak current I_L are given by

$$\begin{array}{rcl} I_{Na} & = & g_{Na}m^3h(V - V_{Na}), \\ I_K & = & g_K n^4(V - V_K), \\ I_L & = & g_L(V - V_L), \end{array} \tag{2.4}$$

with constant conductances $g_{Na} = 120\text{mS/cm}^2$, $g_k = 36\text{mS/cm}^2$, $g_L = 0.3\text{mS/cm}^2$, the potentials $V_{Na} = 50\text{mV}$, $V_K = -77\text{mV}$, $V_L = -54.4\text{mV}$ and the gating variables m, h, n. The gating variables are governed by differential equations of the form (2.2), namely

$$\begin{array}{rcl} \dot{m} & = & \alpha_m(V)(1 - m) - \beta_m(V)m, \\ \dot{h} & = & \alpha_h(V)(1 - h) - \beta_h(V)h, \\ \dot{n} & = & \alpha_n(V)(1 - n) - \beta_n(V)n, \end{array} \tag{2.5}$$

with the normalized functions

$$\begin{array}{rcl} \alpha_m(V) & = & 0.1(V + 40)/(1 - \exp(-(V + 40)/10)), \\ \beta_m(V) & = & 4\exp(-(V + 65)/18), \\ \alpha_h(V) & = & 0.07\exp(-V + 65)/20, \\ \beta_h(V) & = & 1/(1 + \exp(-(V + 35)/10)), \\ \alpha_n(V) & = & 0.01(V + 55)/(1 - \exp(-(V + 55)/10)), \\ \beta_n(V) & = & 0.125\exp(-(V + 65)/80). \end{array} \tag{2.6}$$

The voltage V in Eq. (2.6) is in mV. The gating variables as well as the function values of the transition rates (2.6) are dimensionless.

2.3 Similar models

There are many other models of cells and fibers that are based on the Hodgkin-Huxley formalism. One of the most well-know models of this type, namely the Morris-Lecar model [13], arose from studies of the excitability of the barnale muscle fiber. The model takes ionic currents resulting from potassium ions (K^+) and calcium ions (Ca^+) into account. The channels' behaviour is modelled by $p = 2$ gating variables. Overall, the model has the dimension $n = 3$. Under some circumstances, the model can be reduced further to the dimension $n = 2$ (see [13]).

Several system-theoretical approaches have been used to reduce the dimension of the Hodgkin–Huxley model. For example, FitzHugh [14] observed that the spike-like oscillations of the Hodgkin-Huxley model are similar to oscillations generated by the Bonhoeffer-van der Pol equation [15]. An equivalent circuit model using a tunnel diode was derived in [16]. As a whole, the FitzHugh–Nagumo model has the dimenion $n = 2$.

In the past, the low dimensional models have been simulated on analog computers. Today fast digital computers allow the simulation of significantly more complicated models. During the last decades, several advanced models have been developed. The Connor–Stevens model [17] takes $p = 5$ gating variables into account and is therefore 6-dimensional. Another widely used model was derived by Traub [18, 19] and is 5-dimensional. Further informations on the modelling of excitable cells etc. can be found in [11, 20, 21].

3 Observer Based Residuum Generation

3.1 Observer structure

The 4-dimensional Hodgkin–Huxley model (2.3)-(2.5) can be written as

$$\begin{aligned} \dot{V} &= f(V,w) + \tfrac{1}{C} I, && \text{(3.1a)} \\ \dot{w} &= g(V,w) && \text{(3.1b)} \end{aligned}$$

with smooth nonlinear maps $f : \mathbb{R} \times \mathbb{R}^3 \to \mathbb{R}$, $g : \mathbb{R} \times \mathbb{R}^3 \to \mathbb{R}^3$, and $w = (m,h,n)^T$. To estimate the unknown input current I via the measured voltage V we consider the following dynamic system:

$$\begin{aligned} \dot{\hat{V}} &= f(\hat{V},\hat{w}) + k(V - \hat{V}), && \text{(3.2a)} \\ \dot{\hat{w}} &= g(V,\hat{w}), && \text{(3.2b)} \\ \tilde{V} &= V - \hat{V}. && \text{(3.2c)} \end{aligned}$$

The first part (3.2a),(3.2b) is a high-gain observer for (3.1), where the constant observer gain $k > 0$ acts only on the first subsystem (3.2a). A difference to standard high-gain observers is the direct injection of the measured voltage V into the second subsystem (3.2b). The output of (3.2) is the observation output error $\tilde{V}$ given in Eq. (3.2c). As a whole, system (3.2) has the structure of an observer based residual generator used for fault detection (see [9] and references cited there). The observation error is governed by the error dynamics

$$\begin{aligned} \dot{\tilde{V}} &= f(V,w) - f(\hat{V},\hat{w}) - k\tilde{V} + \tfrac{1}{C} I, && \text{(3.3a)} \\ \dot{\tilde{w}} &= g(V,w) - g(V,\hat{w}), && \text{(3.3b)} \\ \tilde{V} &= V - \hat{V}, && \text{(3.3c)} \end{aligned}$$

where $\tilde{w} = w - \hat{w}$.

3.2 Passivity

For a given initial value of (3.1) and a bounded input I, the trajectories of the original system stay in a compact subset $\mathbb{X} \subset \mathbb{R}^n$. Since the map f is continuousely differentiable (see Eqs. (2.3) and (2.4)), it is also Lipschitz continuous on $\mathbb{X}$. We assume that there exist constants $L_1, L_2 > 0$ such that

$$\left| f(V,w) - f(\hat{V},\hat{w}) \right| \leq L_1 \left| V - \hat{V} \right| + L_2 \left\| w - \hat{w} \right\|$$

holds on $(V,w), (\hat{V},\hat{w}) \in \mathbb{X}$, where $|\cdot|$ is the absolute value and $\|\cdot\|$ is the euclidean norm.

In contrast to classical observer design we are not directly interested in the stability of the error dynamics (3.3), but in its input-output behaviour. Instead, we will describe the input-output behaviour qualitatively using the concept of passivity [22]. The candidate storage function

$$S(\tilde{V},\tilde{w}) = \frac{C}{2}\tilde{V}^2 + \frac{1}{2}\sum_{i=1}^{p} \tilde{w}_i^2$$

is positive definite and radially unbounded. The derivative along the error dynamics (3.3) reads as

$$\dot{S}(\tilde{V},\tilde{w})\Big|_{(3.3)} = C\tilde{V}\dot{\tilde{V}} + \sum_{i=1}^{p} \tilde{w}_i\dot{\tilde{w}}_i. \tag{3.4}$$

For the first summand of (3.4) we obtain

$$\begin{aligned} C\tilde{V}\dot{\tilde{V}} &= C\tilde{V}\left(f(V,w) - f(\hat{V},\hat{w}) - k\tilde{V} + \tfrac{1}{C}I\right) \\ &\leq C\tilde{V}\left|f(V,w) - f(\hat{V},\hat{w})\right| - Ck\tilde{V}^2 + \tilde{V}I \\ &\leq CL_1\tilde{V}\left|\tilde{V}\right| + CL_2\tilde{V}\left\|\tilde{w}\right\| - Ck\tilde{V}^2 + \tilde{V}I \\ &\leq CL_1\tilde{V}^2 + \theta CL_2\tilde{V}^2 + CL_2\theta^{-1}\left\|\tilde{w}\right\|^2 - Ck\tilde{V}^2 + \tilde{V}I \\ &= C\left(L_1 + \theta L_2 - k\right)\tilde{V}^2 + CL_2\theta^{-1}\left\|\tilde{w}\right\|^2 + \tilde{V}I \end{aligned}$$

for any $\theta > 0$ because $ab \leq \theta a^2 + \theta^{-1}b^2$ for all $a, b \in \mathbb{R}$. Taking the special form (2.2) of subsystem (3.3b) into account, the second summand of (3.4) is bounded by

$$\sum_{i=1}^{p} \tilde{w}_i\dot{\tilde{w}}_i = -\sum_{i=1}^{p} \left(\alpha_i(V) + \beta_i(V)\right)\tilde{w}_i^2 \leq -\mu\left\|\tilde{w}\right\|^2 \tag{3.5}$$

with

$$\mu := \inf_{i,V} \left(\alpha_i(V) + \beta_i(V)\right) > 0$$

since the functions α_i and β_i are positive and the measured voltage in bounded. Altogether we obtain

$$\begin{aligned} \dot{S}(\tilde{V},\tilde{w})\Big|_{(3.3)} &\leq -C\left(k - L_1 - \theta L_2\right)\tilde{V}^2 - \left(\mu - CL_2\theta^{-1}\right)\left\|\tilde{w}\right\|^2 + I\tilde{V} \\ &\leq -\rho\tilde{V}^2 - \nu\left\|\tilde{w}\right\|^2 + I\tilde{V}, \end{aligned}$$

where $\rho := C(k - L_1 - \theta L_2)$ and $\nu := \mu - CL_2\theta^{-1}$. Choosing $\theta > CL_2/\mu$ and $k > L_1 + \theta L_2$ yields $\rho, \nu > 0$. For $I = 0$, the scalar field S is a Lyapunov function, i.e., the point $\tilde{V} = 0$, $\tilde{w} = 0$ is a globally asymptotically stable equilibrium. However, we also have

$$\dot{S}(\tilde{V})\Big|_{(3.3)} \leq -\rho\tilde{V}^2 + I\tilde{V},$$

which implies that the error system (3.3) is not only passive, but also output feedback passive [22] with respect to the input I and the output $\tilde{V}$. Physically, the supply rate $I\tilde{V}$ is the difference of electric power of systems (3.1) and (3.2) provided by the input current source, i.e., the rate of increase of energy is not bigger than the input power.

3.3 Input reconstruction

The residual $\tilde{V}$ generated by (3.2) describes the degree of consistency between the model (3.1) and the observer scheme (3.2). Since the input current is missing in (3.2a), one would expect that the residual $\tilde{V}$ is somehow related to the unknown input I. In the classical application of residual generators, namely in fault detection, the residual is

only used qualitatively to indicate that a fault occurred (and which one). Here, we want to use the residual $\tilde{V}$ quantitatively to obtain an estimate of the input current I.

From Eq. (3.5) we conclude that the equilibrium $\tilde{w} = 0$ of subsystem (3.3b) is globally asymptotically stable (uniform in V). After the transient oscillations of (3.3) we can expect $\tilde{w} \approx 0$, i.e., $w \approx \hat{w}$. To ensure the passivity of (3.3), we have to choose $k > 0$ sufficiently large. This implies

$$\left| f(V, w) - f(\hat{V}, w) \right| \ll k \left| \tilde{V} \right| \quad \text{for} \quad t \gg 0, \tag{3.6}$$

which means that the observer correction term is much stronger than the difference between the two systems (3.1) and (3.2).

Next, we consider Eq. (3.3a) near an equilibrium point, i.e., $\dot{\tilde{V}} \approx 0$. From (3.6) we conclude that

$$0 \approx -k\,\tilde{V} + \frac{1}{C} I.$$

Hence, an estimate of the input current I can be obtained from $\tilde{V}$ by

$$I \approx k\,C\,\tilde{V}. \tag{3.7}$$

If the current input I exceeds a certain level, the original system (3.1) oscillates. These oscillations can also be seen at the output $\tilde{V}$ of (3.2), although the oscillations are better suppressed using a large observer gain k. Therefore, we will smooth the current estimate from (3.7) by a mth order low-pass with the continuous time transfer function

$$F(s) = \frac{1}{(1 + sT)^m}$$

with a time constant $T > 0$. For simplicity, the transfer function used here has a multiple real pole at $-1/T$. However, one could also choose from several other filter design techniques (e.g. Bessel, Butterworth or Cauer filter). Combining time and frequency domain as well as taking the scaling (3.7) into account, the final estimate $\hat{I}$ of I results from

$$\hat{I}(t) = \frac{k\,C}{(1 + sT)^m} \circ \tilde{V}(t). \tag{3.8}$$

The whole estimation scheme is given in Fig. 3.1.

4 Simulation Results

For the simulation of the Hudgkin–Huxley model (2.3)-(2.6) we used the initial values $V(0) = 65\text{mV}$, $m(0) = 0.1$, $h(0) = 0.6$ and $n(0) = 0.3$. The input current was chosen as follows:

$$I(t) = \begin{cases} 10\mu\text{A/cm}^2 & \text{for} \quad 0\text{ms} \le t < 80\text{ms}, \\ 25\mu\text{A}/cm^2 & \text{for} \quad 80\text{ms} \le < 140\text{ms}, \\ 15\mu\text{A}/cm^2 & \text{for} \quad t \ge 140\text{ms}. \end{cases} \tag{4.1}$$

The simulation was carried out by the scientific software package Scilab [23]. The generated output trajectory is shown in Fig. 4.1. The membrane voltage shows spike-like oscillations, whose amplitude and frequency vary according to the current in the specific time interval.

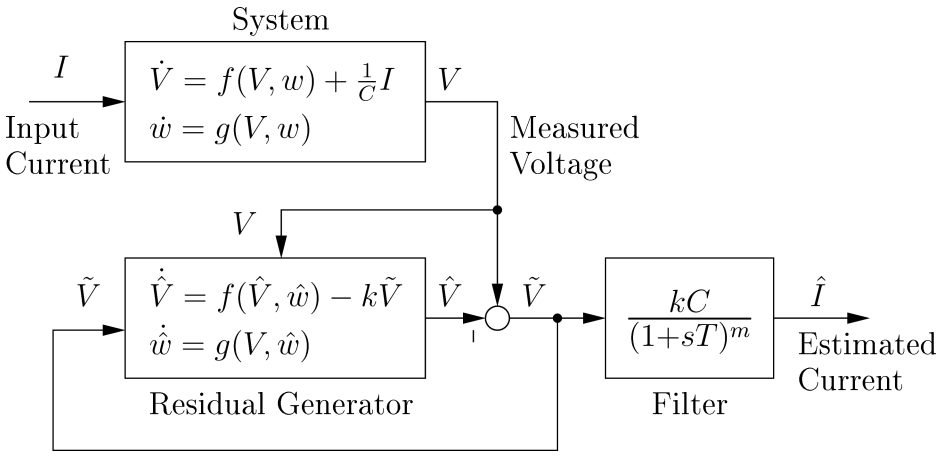

Figure 3.1: Current Estimation Scheme.

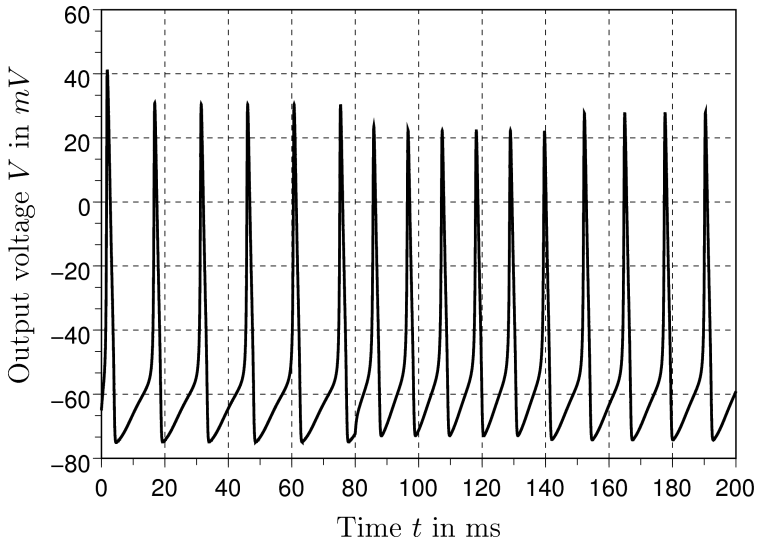

Figure 4.1: Output voltage of the Hudgkin–Huxley model (2.3)-(2.6).

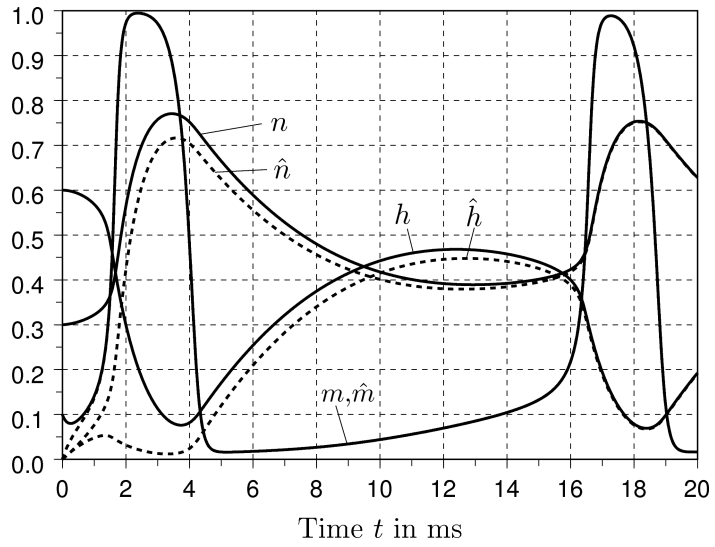

Figure 4.2: Trajectories of the gating variables and its estimates.

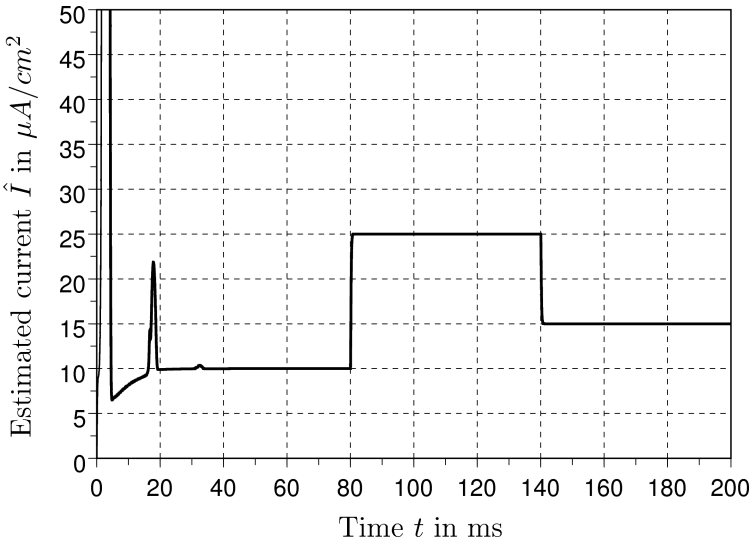

Figure 4.3: Estimated current $\hat{I}$ according to Eq. (3.8).

For the observer (3.2a) we have chosen the initial value $\hat{V}(0) = V(0) = 65\text{mV}$ to be consistent with the measurement (see [24, Section 3.3]). Since we have no further information on the state of the gating variables we used the 3-dimensional zero vector as initial value of (3.2b), i.e., $\hat{m}(0) = \hat{h}(0) = \hat{n}(0) = 0$. The transient behaviour of the observer (3.2b) for the gating variables is shown in Fig. 4.2. We used solid lines for the original gating variables m, n, h and dashed lines for its estimates $\hat{m}, \hat{h}, \hat{n}$ generated by the observer (3.2b). Note that Fig. 4.2 has a different time domain as Fig. 4.1, i.e., we only show the first 20ms in Fig. 4.2. After that, the gating variables and its estimates basically coincide, i.e., they cannot be separated visually.

The observer scheme (3.2) with the gain $k = 1000$ yields the residual $\tilde{V}$. To obtain an estimate $\hat{I}$ for the current I we have to scale and filter this voltage difference according to Eq. (3.8), where we used the normalized filter time constant $T = 0.1$. The result is shown in Fig. 4.3. After some transient oscillations the estimated current matches the input current (4.1) almost perfectly.

5 Conclusions

We suggested a new approach to estimate the current input into a (possibly living) cell. This method requires a reasonable precise model of the cell under consideration. In contrast to voltage and patch clamp techniques, our approach cannot be used to analyze new cell types or cells with significant anomalies. However, our measurement technique can be used to verify given models and to study the interaction of cells (such as neurons interconnected by synapses).

Acknowledgements

The author thanks Prof. Pranay Goel from the Indian Institute of Science, Education and Research, Pune, who brought this problem to my attention.

References

[1] Purves, D. et al. *Neuroscience*. Sinauer Associates Inc., Sunderland, MA, USA, 3rd edition, 2004.

[2] Finkel, A.S. and Gage, P.W. Conventional voltage-clamping with two intracellular microelectrodes. In Smith et al. [6], pages 47–94.

[3] Cole, K.S. *Membranes, Oins and Impulses: A Chapter of Classical Biophysics*. University of California Press, Berkeley, CA, USA, 1968.

[4] Neher, E. and Sakmann, B. Single-channel currents recorded from membrane denervated frog muscle fibers. *Nature* **260** (1976) 799–802.

[5] Molecular Devices. *The Axon CNS Guide to Electrophysiology and Biophysics Laboratory Techniques*, 1993.

[6] Smith, T.G., Lecar, H., Redman, S.J. and Gage, P.W. editors. *Voltage and patch Clamping with Microelectrodes*. William & Wilkins, 1985.

[7] Goel, P. and Röbenack, K. Observing the current input in neurons. Technical Report 38, Mathematical Biosciences Institute, The Ohio State University, Aug. 2005.

[8] Röbenack, K. and Goel, P. Observer based measurement of the input current into a neuron. *Mediterranean Journal of Measurement and Control* **3**(1) (2007) 22–29.

[9] Nijmeijer, H. and Fossen, T.I. editors. *New Directions in Nonlinear Observer Design*, volume 244 of *Lecture Notes in Control and Information Science*. Springer-Verlag, London, 1999.

[10] Frank, P.M., Ding, S.X. and Marcu, T. Model-based fault diagnosis in technical processes. *Transactions of the Institute of Measurement and Control*, **22**(1) (2000) 57–101.

[11] Hille, B. *Ionic Channels of Excitacle Membranes*. Sinauer, 1992.

[12] Hodgkin, A.L. and Huxley, A.F. A quantitative description of membrane current and its application to conduction and excitation in nerve. *Journal of Physiology* **117** (1952) 500–544.

[13] Morris, C. and Lecar, H. Voltage oscillations in the barnacle giant muscle fiber. *Biophys. J.* **35**(1) (1981) 193–213.

[14] FitzHugh, R. Impulses and physiological states in theoretical models of nerve membrane. *Biophys. J.* **1** (1961) 445–466.

[15] Bonhoeffer, K.F. Activation of passive iron as a model for the excitation of nerve. *Journal of General Physiology* **32** (1948) 69–91.

[16] Nagumo, J., Arimoto, S. and Yoshizawa, S. An active pulse transmission line simulating nerve axon. *Proc. IRE* **50** (1962) 2061–2070.

[17] Connor, J.A. and Stevens, C.F. Prediction of repetitive firing behaviour from voltage clamp data on an isolated neurone soma. *Journal of Physiology* **213** (1971) 31–53.

[18] Traub, R.D. and Miles, R. *Neuronal networks of the hippocampus*. Cambridge University Press, Cambridge, 1991.

[19] Traub, R.D., Jefferys, J.G.R., and Whittington, M.A. *Fast Oscillations in Cortical Circuits*. MIT Press, Cambridge, MA, 1999.

[20] Johnston, D. and Wu, S.M. *Foundations of Cellular Neurophysiology*. MIT Press, Cambridge, MA, 1995.

[21] Rinzel, J. and Ermentrout, B. editors. *Methods in Neuronal Modeling: From Synapses to Networks*. MIT Press, Cambridge, MA, 1998.

[22] Sepulchre, R., Janković, M. and Kokotović, P. *Constructive Nonlinear Control*. London, Springer, 1997.

[23] Gomez, C. *Engineering and Scientific Computing with Scilab*. Birkhauser, Boston, 1999.

[24] Zeitz, M. *Nichtlinear Beobachter für chemische Reaktoren*, volume 27 of *Fortschrittsberichte der VDI-Zeitschriften, Reihe 8, Meß-, Steuerungs- und Regelungstechnik*. VDI-Verlag, Düsseldorf, Germany, 1977.